

Catalytic study and electrochemical promotion of propane oxidation on Pt/YSZ

Christos Kokkofitis, George Karagiannakis, Stergios Zisekas, Michael Stoukides*

Chemical Engineering Department and Chemical Process Engineering Research Institute, University Box 1517, University Campus, Thessaloniki 54124, Greece

Received 18 February 2005; revised 24 June 2005; accepted 14 July 2005

Available online 11 August 2005

Abstract

The Pt-catalyzed oxidation of propane was studied in an oxygen ion conducting solid electrolyte cell at 623–773 K and atmospheric total pressure. Under open circuit, the solid electrolyte potentiometry (SEP) technique was used to monitor the thermodynamic activity of oxygen adsorbed on the catalyst surface during reaction. Reaction kinetics and SEP measurements were combined to elucidate the reaction mechanism. Under certain conditions, sustained oscillations in the reaction rate and the surface oxygen activity were observed. The reaction exhibited a strong non-Faradaic modification of catalytic activity (NEMCA) effect. By varying the potential of the Pt catalyst, the rate of propane oxidation could be reversibly enhanced by up to a factor of 1400. At positive potentials, the reaction exhibited a pronounced electrophobic NEMCA enhancement. At negative potentials, the reaction also exhibited a strong electrophilic enhancement, indicating that the promoting effect is of the “inverted volcano” type.

© 2005 Elsevier Inc. All rights reserved.

Keywords: Propane oxidation on Pt; Solid electrolyte potentiometry; Electrochemical promotion; Rate oscillations

1. Introduction

As an environmentally benign alternative to conventional flame combustion, the catalytic oxidation of hydrocarbons has received considerable attention [1–6]. The catalysts used for combustion are mainly supported noble metals, especially Pt and Pd [5]. Excluding Pd in the case of methane, Pt is considered the most active metal for the catalytic oxidation of hydrocarbons [3,6].

Stable lower alkanes, such as propane, require relatively high temperatures for complete oxidization over supported Pt catalysts [6]. But if the reaction is run under the appropriate conditions, then the incomplete oxidation of propane can result in the production of industrially important compounds. Toward this end, numerous investigators have studied the Pt-catalyzed oxidative dehydrogenation of propane at high reaction temperatures (873–1373 K). These studies

have focused on the production of propylene, a key chemical in the polymerization and organic synthesis industries [7–9].

Platinum is the most widely used catalyst for the combustion of propane [1–6,10–17]. In an effort to enhance the catalytic activity of Pt, earlier work has focused on the role of the support [4–6,10–12], the effect of particle size and catalyst dispersion [2,3,11], and the effects of solid additives and gas phase promoters [3,13–17].

Yazawa et al. [5] studied the Pt-catalyzed combustion of propane on several supports (MgO, La₂O₃, Al₂O₃, Si₂O₃–Al₂O₃, ZrO₂, and SO₄^{2–}–ZrO₂). They concluded that support materials affect the catalytic activity of Pt by affecting the oxidation state of the catalyst. These authors also observed that the support effect in a reducing atmosphere was significantly different from that in an oxidizing atmosphere. Kiwi-Minsker et al. [4] studied the reaction on Pt supported on glass fiber materials modified by several oxides (Al₂O₃, ZrO₂, and TiO₂) and observed the highest catalytic activity on glass fibers modified by TiO₂. Garetto et al. [6] studied

* Corresponding author. Fax: +30-2310-996145.

E-mail address: stoukidi@cperi.certh.gr (M. Stoukides).

the reaction on zeolite supports and found that their activity was much higher than that of the Pt/Al₂O₃ catalysts. The Pt/zeolites' superiority was attributed to their ability to maintain a higher density of propane at the metal–support interface [6].

Hubbard et al. [2] reported that the catalytic activity of highly dispersed Pt was one to two orders of magnitude higher on Pt/zirconia than on Pt/ γ -alumina. With increasing metal loading, this difference gradually vanished. Yazawa et al. [11] studied the effect of catalyst dispersion on several support materials and found that the reaction turnover frequency decreased with increasing catalyst dispersion and the turnover frequency increased with increasing acid strength of the support. The variation in activity with catalyst dispersion and support acidity was attributed to the concomitant variation in the oxidation state of platinum. Large platinum particles are less oxidized than small ones, and reduced platinum is the much more active form. Similarly, platinum on acidic supports is less oxidized than platinum on basic supports.

The additive effect on supported Pt catalysts has been studied in an effort to find ways to enhance their catalytic activity [10,15,16]. Yazawa et al. [10,16] investigated the variation in reaction rate with the addition of a large number of metal additives on Pt/Al₂O₃ and found that intrinsic catalytic activity increased with increasing electronegativity of the additive. This effect was observed in an oxidizing atmosphere only and was attributed to increased oxidation resistance of Pt [10].

Several investigators have reported that small amounts of SO₂ can promote the catalytic combustion of propane over Pt/Al₂O₃ [3,13,14,17]. Researchers from the University of Cambridge and Ford Motor Co. jointly studied the role of SO₂ in the promotion of Pt/Al₂O₃ catalysts [3]. Their work confirmed that PtO₂ particles are essentially inactive and that an increase in metal loading increases the metallic character of Pt. These findings explain the structural sensitivity of propane combustion. Moreover, sulfation causes simultaneous reduction and partial sintering of the PtO₂ particles. Finally, the effect of SO₂ is not confined to the catalyst itself; it is support-specific because it facilitates the dissociative chemisorption of propane at the Pt/Al₂O₃ interface [3]. Burch et al. [13] studied the reaction on supported Pt catalysts in the presence and in the absence of SO₂. The presence of SO₂ resulted in strongly enhanced activity of the alumina-supported catalysts but produced no effect on the silica-supported catalysts. It has been suggested that SO₂ results in the polarization of the perimeter sites at the Pt–support interface, sites important in the activation of the first C–H bond of propane [13].

Despite the different interpretations presented by the various research groups, it is generally understood that the intrinsic catalytic activity of Pt toward propane oxidation can be significantly enhanced by a properly chosen support and the presence of additives and gas phase promoters. Another alternative approach to catalytic promotion, non-Faradaic

modification of catalytic activity (NEMCA), or electrochemical promotion, has been developed and applied in numerous catalytic reaction systems [18,19]. In NEMCA, the catalytic reaction is run in an electrochemical cell in which one of the electrodes is placed concomitant with the catalyst under study. By appropriately controlling either the current or the cell potential, ions can be “pumped” into or away from the electrode catalyst. Ionic “pumping” changes the work function of the electrode and thus alters its catalytic properties.

Vernoux et al. [20] investigated the electrochemical promotion in the oxidation of propane on Pt, along with the oxidation of propylene. They found significant differences in the promotion behaviors of propane and propylene, and attributed these differences to the much stronger adsorption of the alkene on the catalyst surface. Kotsionopoulos and Bebelis [21] studied the NEMCA effect in the catalytic oxidation of propane on Pt and compared the results with those obtained on Rh. These authors found that the increase in the rate of oxygen consumption could exceed the rate of oxygen ion “pumping” by three orders of magnitude, resulting in enhancement of the intrinsic catalytic rate by up to a factor of 1350 [21].

This work reports results of the reaction of propane oxidation studied in a solid electrolyte cell. Experimental findings obtained under both open- and closed-circuit operation are presented. Under open circuit, the cell operated as a regular catalytic reactor, and the kinetics of the reaction were studied in conjunction with measurements of cell potential. The effect of oxygen ion “pumping” on the catalytic activity of Pt was investigated under closed circuit.

2. Experimental

The experimental apparatus (schematically illustrated in Fig. 1) consisted of the feeding unit, reactor, and analytical system. Reactant gases, C₃H₈, O₂, and diluent He were of 99.999% purity. Analyses of the inlet (C₃H₈ and O₂) and outlet gases (C₃H₈, O₂, CO₂, and H₂O) were performed using a Shimadzu GC-14B on-line gas chromatograph with a thermal conductivity detector. A Porapak QS column was used to separate C₃H₈, CO₂, and H₂O, and a Molecular Sieve 13X was used to separate O₂. CO and CO₂ concentrations were also continuously monitored using a Binos infrared CO and CO₂ analyzer. Constant currents and voltages across the cell were imposed using a 2053 AMEL Galvanostat-Potentiostat. Two multimeters were also used to measure the potential or the current through the cell. The reactor was located in a furnace, the temperature of which was controlled within ± 2 K from the setpoint.

The catalytic and electrocatalytic experiments were carried out in a solid electrolyte cell reactor, shown in Fig. 2. The cell reactor consisted of an 8 mol% yttria-stabilized zirconia (YSZ) tube (15 cm long, 16 mm i.d., 19 mm o.d.), closed at its bottom end. Under the conditions of the present

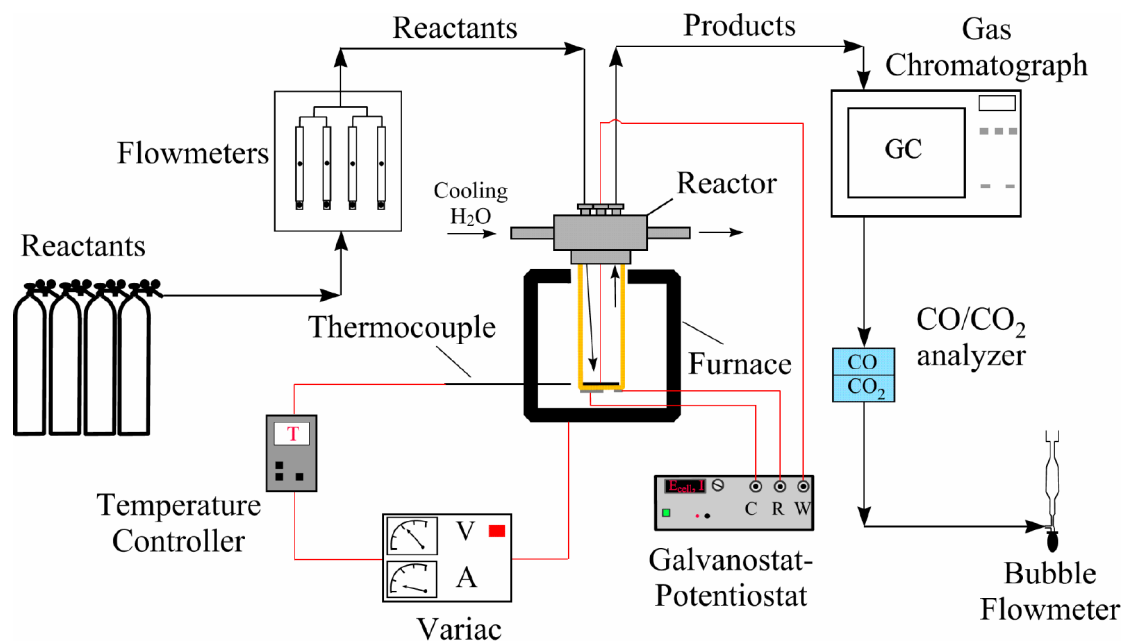


Fig. 1. Schematic diagram of the experimental apparatus.

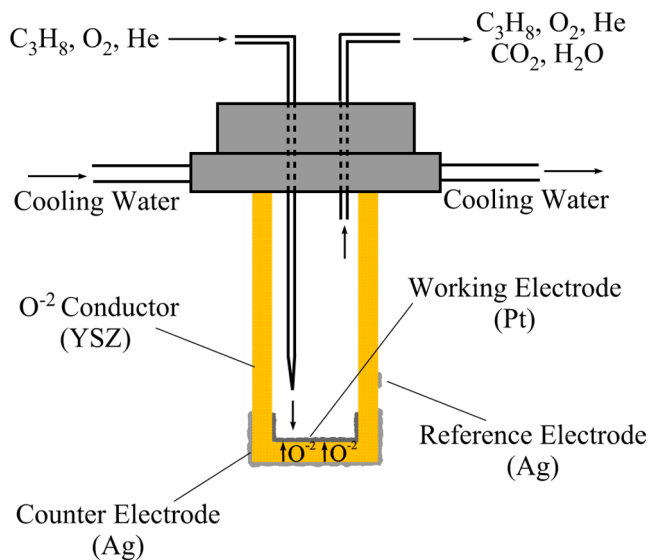


Fig. 2. Schematic diagram of the solid electrolyte cell-reactor.

experiments, this material is a pure oxygen ion (O^{2-}) conductor.

2.1. Catalyst (electrode) preparation and characterization

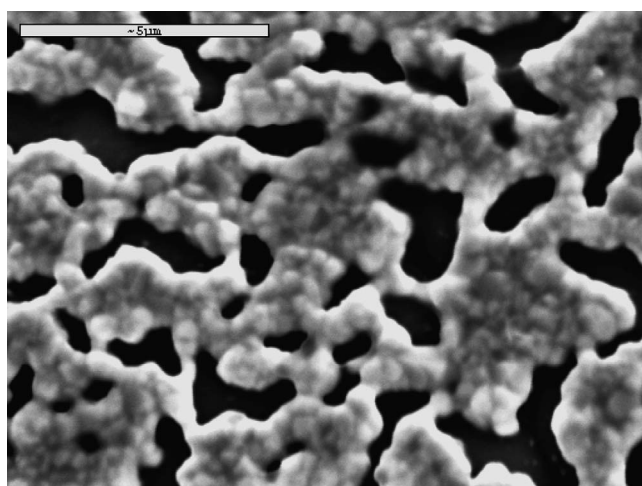
The Pt catalyst electrode was deposited at the inside bottom of the YSZ tube. Similarly, the Ag counter and reference electrodes were deposited on the outer side of the tube and exposed to the ambient air (Fig. 2). Gold wires were used to connect the three electrodes to the instruments. The wires were enclosed in quartz tubes, to avoid contact with the metallic parts of the reactor.

The polycrystalline porous Pt film was prepared from a Pt paste (Engelhard A1121). The electrode was calcined in

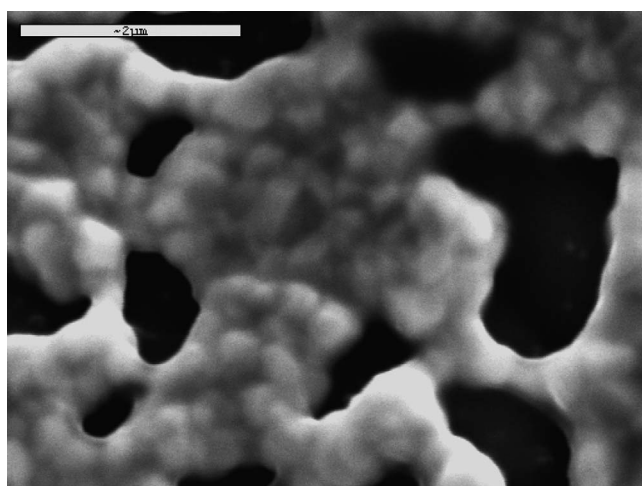
air for 90 min at 1073 K. Scanning electron micrographs of the Pt electrode are shown in Figs. 3 and 4. Figs. 3a and b show a freshly prepared catalyst at $\times 9000$ and $\times 20,000$ magnification, respectively. Fig. 4 shows a Pt electrode that has been exposed for 3 days to a reacting gaseous mixture ($p_{\text{C}_3\text{H}_8} = 1 \text{ kPa}$, $p_{\text{O}_2} = 1 \text{ kPa}$, and $p_{\text{He}} = 98 \text{ kPa}$, $T = 823 \text{ K}$) at $\times 3000$ magnification. Under these conditions, the catalyst underwent severe deactivation due to carbon deposition on the Pt surface, as verified by EDS analysis of the samples. Fig. 4 clearly shows very large crystallites of carbon formed on the Pt surface. The problem of carbon deposition was insignificant when the reactor temperature was kept below 773 K.

Three cell reactors (R_1 , R_2 , and R_3), with different catalytic surface areas, were used in the present experiments. For R_2 , the catalyst loading was 8 mg of Pt. Using this amount and an average particle size of $1 \mu\text{m}$ (Fig. 3), a surface area of 23 cm^2 was calculated. The surface areas for R_1 and R_3 were calculated by comparing reaction rates obtained with these reactors to the reaction rate obtained with R_2 at the same reaction conditions. Thus the active catalytic surface areas for R_1 and R_3 (before deactivation for R_3) were 1480 and 450 cm^2 , respectively. The deactivated R_3 exhibited a 300-fold decrease in catalytic activity. The superficial electrode surface area was the same for all three catalyst electrodes, about 3 cm^2 .

The Ag counter and reference electrodes were prepared from a Ag paste (GC Electronics no. 22-202). Silver was used as the auxiliary electrode material, because it adheres very strongly to the zirconia outside surface. The two electrodes were calcined in air for 1 h at 923 K. The superficial surface areas of the counter and the reference electrode were 5.5 and 0.6 cm^2 , respectively.



(a)



(b)

Fig. 3. Scanning electron micrographs of a freshly prepared Pt catalyst-electrode: (a) at $\times 9000$ magnification and (b) at $\times 20,000$ magnification.

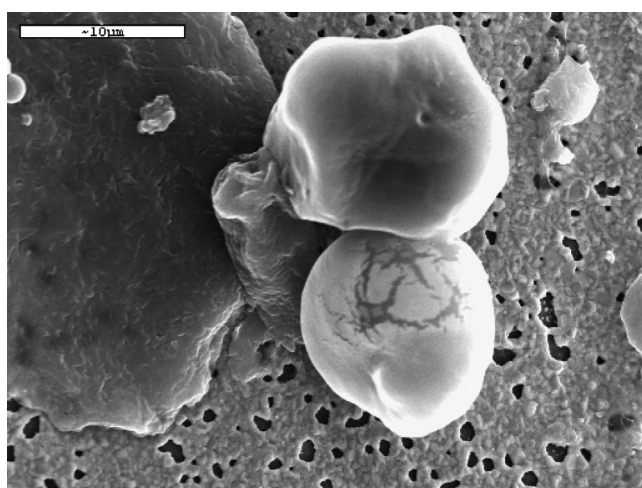


Fig. 4. Scanning electron micrographs of a deactivated Pt electrode exposed for 3 days to reaction conditions ($p_{\text{C}_3\text{H}_8} = 1$ kPa, $p_{\text{O}_2} = 1$ kPa, $p_{\text{He}} = 98$ kPa, $T = 823$ K) at $\times 3000$ magnification.

2.2. Electrochemical techniques and measurements

Under open circuit (i.e., with no current passing through the solid electrolyte), and when both reactants were co-fed as gaseous C_3H_8 and O_2 , the cell reactor of Fig. 2 operated as a regular catalytic reactor. In that case, the catalytic reaction rate measurements were combined with potentiometric data using the solid electrolyte potentiometry (SEP) technique. The principle of SEP is simple: One of the electrodes is exposed to the reacting mixture and thus serves as a catalyst for the reaction under study, whereas the other electrode is exposed to the air and serves as a reference electrode. It has been shown [18,19,22,23] that the thermodynamic activity of atomic oxygen adsorbed on the catalyst surface is given by the equation

$$\alpha_o = (0.21)^{1/2} \exp(2FE/RT), \quad (1)$$

where F is the Faraday constant, R is the ideal gas constant, T is the absolute temperature, E is the electromotive force (emf) of the cell, and α_o is the thermodynamic activity of atomically adsorbed oxygen. The validity of Eq. (1) is based on several assumptions [18,22,23], most important of which is that atomically adsorbed oxygen is the only species to equilibrate rapidly with oxygen ions at the gas–electrode–electrolyte interline. Although certainly valid for the reference electrode, this assumption may not hold true for the working electrode. Originally proposed by Wagner [24], SEP was first applied in the study of SO_2 oxidation [25] and since then has been used in conjunction with kinetic measurements in many catalytic oxidation reactions [19,22,23]. SEP has two advantages: (a) it is an in situ technique, and (b) the measurement is continuous. The latter is very helpful in examining transient or oscillatory phenomena on catalytic surfaces. Earlier SEP studies were conducted on metal electrodes but later the technique was extended into oxide electrodes [22].

Under closed circuit, the cell reactor of Fig. 2 can operate as an electrochemical oxygen “pump.” Using an external power source, a current (I) can be imposed through the oxygen ion (O^{2-}) conducting solid electrolyte. This current corresponds to a flux of $I/2F$ g atoms of O_2/s . Electrochemically “pumped” oxygen can alter the catalytic properties of the electrode catalyst. In early studies, in which the total amount of oxygen required for the reaction was supplied electrochemically, the maximum attainable rate of oxygen consumption at the anode was equal to the rate of O^{2-} transport [18]. This is the case of *Faradaic* operation. But if gaseous O_2 were co-fed with reactants in the gas phase, then it would be possible for the rate of oxygen consumption to exceed the rate of electrochemical transport of oxygen. Vayenas et al. [18,19] defined the rate enhancement factor Λ as

$$\Lambda = \Delta r / (I/2F), \quad (2)$$

where Δr is the increase in the rate of oxygen consumption and $I/2F$ is the imposed flux of O^{2-} through the elec-

trolyte, both in g atoms O_2/s . If $\Lambda = 1$, then the effect is Faradaic. In many studies reported thus far, however, values of Λ greatly exceeding unity (as high as 10^5) have been observed [19]. This phenomenon, termed non-Faradaic electrochemical modification of catalytic activity (NEMCA), has been attributed to changes in the catalyst work function caused by oxygen pumping [18,19]. In addition to the Λ factor, Vayenas et al. defined another dimensionless parameter ρ as

$$\rho = r/r_o, \quad (3)$$

where r is the catalytic reaction rate obtained under “pumping” and r_o is the open-circuit catalytic rate (i.e., at $I = 0$). Today it is well established that the NEMCA phenomenon is due to electrochemically imposed spillover of ions from the solid electrolyte to the electrode catalyst surface, and it is these ions that act as promoters for the catalytic reactions [19].

3. Results

3.1. Catalytic (open-circuit) measurements

The catalytic reaction rate and the surface oxygen activity behavior was studied at 623–773 K and at 100 kPa total pressure. The partial pressure of inlet propane ranged from 0.2 to 1.7 kPa, and that of oxygen ranged from 0.15 to 10.0 kPa. Helium was used as the diluent, and the total volumetric flow rate was approximately $90 \text{ cm}^3/\text{min}$. As shown previously [26,27], the reactor behavior is very close to that of an ideal CSTR for the foregoing volumetric flow rates. At all temperatures and reactant compositions examined, under open- or closed-circuit operation, the only reaction products detected were CO_2 and H_2O . Hence in all of the results reported herein, reaction rate is expressed in mol of propane consumed per second.

Reactor R_1 was used in the open-circuit experiments. The extent of noncatalytic oxidation of propane was investigated using a “blank” YSZ tube, identical to those used as cell reactors. Propane and oxygen passed through the blank reactor at partial pressures and temperatures similar to those used for the catalytic studies. It was found that the noncatalytic reaction rates were about 2–3% of the total reaction rate at the highest temperature examined (823 K). The kinetic results presented herein have been corrected by subtracting the noncatalytic contribution.

Fig. 5 shows the dependence of the reaction rate and the surface oxygen activity on the partial pressure of propane, $p_{C_3H_8}$. The partial pressure of oxygen, p_{O_2} , was kept at 3 kPa, and the temperature varied from 623 to 773 K. Fig. 5a shows that the reaction rate increases slowly with propane up to a certain $p_{C_3H_8}$, above which a sharper rate increase is observed. This change in the slope of rate versus $p_{C_3H_8}$ is not observed at 623 K. The corresponding α_o values shown

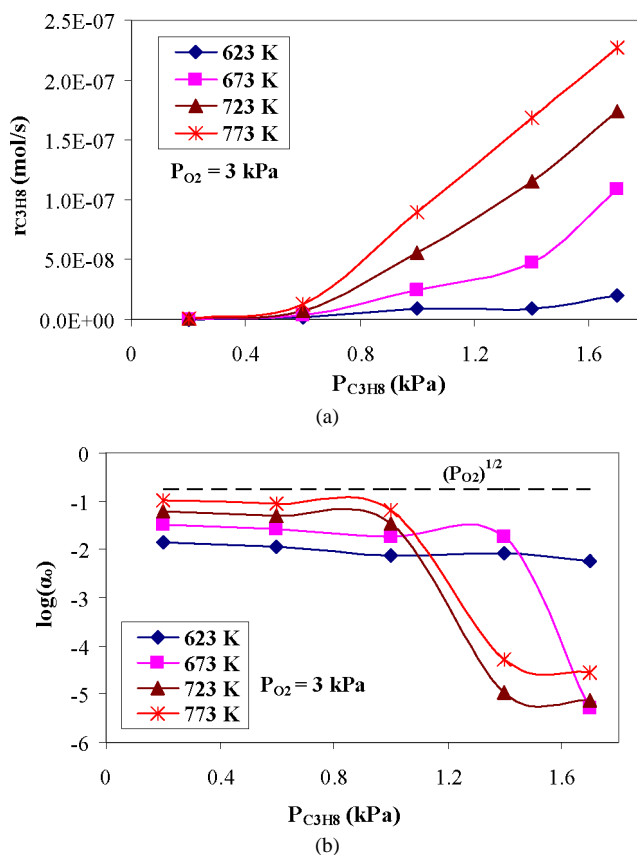


Fig. 5. Dependence of (a) the reaction rate and (b) the surface oxygen activity on $p_{C_3H_8}$ at various reaction temperatures. $p_{O_2} = 3 \text{ kPa}$, reactor R_1 .

in Fig. 5b, vary from 10^{-1} to 10^{-6} and decrease with increasing propane. The horizontal dotted line above the α_o data corresponds to the gas phase $p_{O_2}^{1/2}$ values in the reactor. If thermodynamic equilibrium were established between adsorbed and gaseous oxygen, then the α_o data should fall on the dotted line. It can be seen that the α_o values are lower than the $p_{O_2}^{1/2}$ values. It is also noteworthy that a sharp increase in the reaction rate above a threshold $p_{C_3H_8}$ (e.g., $p_{C_3H_8} > 0.85 \text{ kPa}$ at $T = 723 \text{ K}$) is accompanied by an up to four orders of magnitude decrease in α_o . At 623 K, where there seems to be no change in the slope of the reaction rate curve, no sharp decrease in the α_o is observed either.

Figs. 6a and b show the dependence of reaction rate and surface oxygen activity, respectively, on p_{O_2} . The partial pressure of propane was kept at 1 kPa, and the temperature was varied from 623 to 773 K. Fig. 6a shows that at low p_{O_2} , the reaction rate increases drastically until a maximum value is attained. Then the reaction rate decreases sharply, and at even higher p_{O_2} , the reaction rate levels off to low values. Fig. 6b shows that at p_{O_2} where the reaction rate maxima are observed, the surface oxygen activity attains very low values. As in Fig. 5b, the dotted line above the α_o data in Fig. 6b corresponds to the gas phase $p_{O_2}^{1/2}$ values in the reactor. Clearly, at low p_{O_2} where the reaction rate is higher, the deviation from equilibrium between adsorbed and gaseous

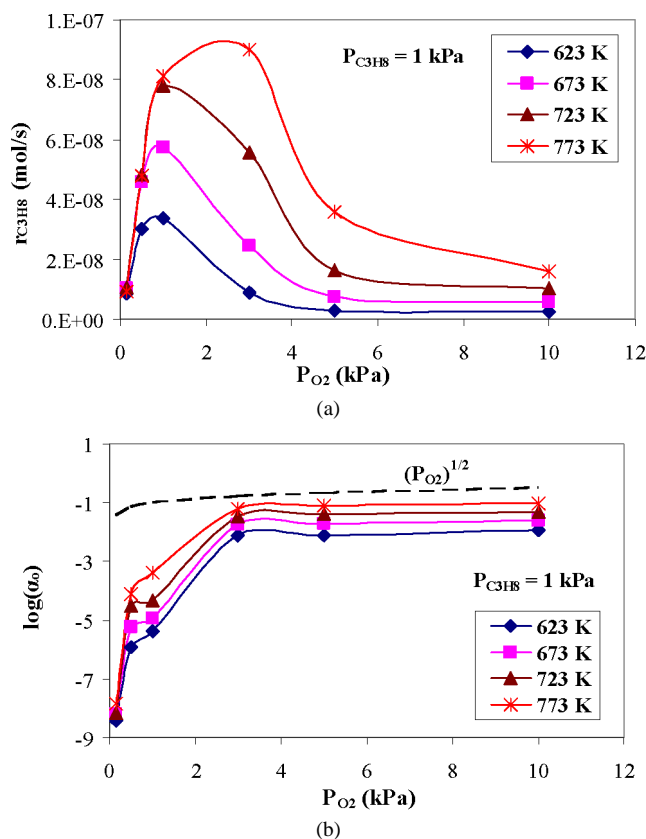


Fig. 6. Dependence of (a) the reaction rate and (b) the surface oxygen activity on p_{O_2} at various reaction temperatures. $p_{C_3H_8} = 1$ kPa, reactor R₁.

oxygen is much stronger. At high p_{O_2} , where very low reaction rates are observed, the difference between α_o and $p_{O_2}^{1/2}$ values is diminished.

3.2. Closed-circuit measurements

Figs. 7–12 contain data obtained with the cell operating under closed circuit. Reactors R₂ and R₃ were used in these experiments; the data of Figs. 7–9 were obtained with R₂ and those of Figs. 10–12 were obtained with reactor R₃. Figs. 7a and b show typical galvanostatic transients; that is, they depict the transient effect of imposed current (I) on the rate of propane oxidation. Fig. 7a shows the effect of positive current, which corresponds to a flux of oxygen ions “pumped” to the catalyst. At $t < 0$, the circuit is open ($I = 0$) and steady state has been established. The catalyst temperature is maintained at 623 K, and the inlet partial pressures of propane and oxygen are both kept at 1 kPa. The steady-state open-circuit reaction rate is 2.05×10^{-10} mol C₃H₈/s, which corresponds to an oxygen consumption rate $r_o = 2.05 \times 10^{-9}$ g atoms O₂/s. At $t = 0$, a constant current $I = +0.15$ mA is imposed which corresponds to an oxygen flux equal to $I/2F = 7.8 \times 10^{-10}$ g atoms O₂/s. The reaction rate gradually increases to attain a new steady-state value of $r = 6.5 \times 10^{-8}$ g atoms O₂/s, about 32 times higher than the open-circuit rate (r_o). On in-

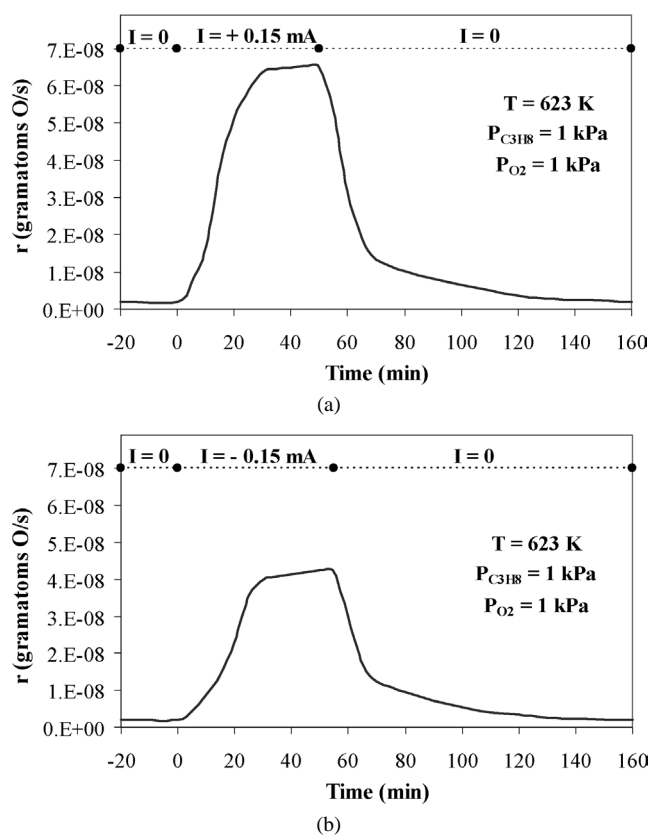


Fig. 7. Propane oxidation rate response to step changes in applied (a) positive ($I = +0.15$ mA) and (b) negative ($I = -0.15$ mA) current. $T = 623$ K, $p_{C_3H_8} = 1$ kPa, $p_{O_2} = 1$ kPa, reactor R₂.

terruption of the current, the reaction rate gradually returns to its open-circuit value. As shown in Fig. 7b, a qualitative similar behavior is observed on imposing a negative (oxygen ions being “pumped” away from the catalyst) current $I = -0.15$ mA, which corresponds to an oxygen flux equal to $I/2F = -7.8 \times 10^{-10}$ g atoms O₂/s. Again, an increase in the reaction rate is observed. The maximum level-off value is about $r = 4.2 \times 10^{-8}$ g atoms O₂/s, about 21 times higher than the open-circuit rate (r_o). When the current is interrupted, the open-circuit value of reaction rate is gradually restored.

Fig. 8 presents galvanostatic steady-state results. The absolute value of the Faradaic efficiency, $|A| = |I|/2F$, is plotted versus the oxygen flux $I/2F$, imposed either toward (positive I) or away from (negative I) the catalyst. The data points correspond to steady states. At positive currents, $|A|$ increases drastically with $I/2F$ to reach a maximum value of 90. At higher $I/2F$, $|A|$ decreases gradually to a value of 20. The same shape of curve is obtained at negative currents.

Figs. 9a, b, and c show the effect of V_{WR} , the electrical potential difference between the working and reference electrode, on the change in the reaction rate $\Delta r = (r - r_o)$, the dimensionless parameter ρ , and the absolute value of A , respectively. At all temperatures examined, an increase in

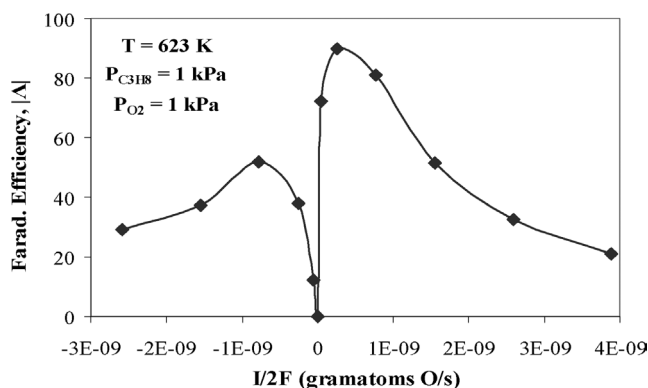


Fig. 8. Dependence of the absolute Faradaic efficiency $|A|$, on the electrochemical oxygen ion supply $I/2F$. $T = 623$ K, $p_{C_3H_8} = 1$ kPa, $p_{O_2} = 1$ kPa, reactor R_2 .

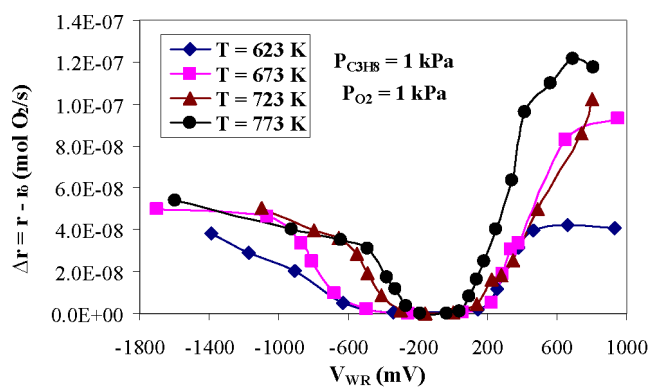
reaction rate is observed at either positive or negative V_{WR} . A positive V_{WR} corresponds to positive current, that is, oxygen ions “pumped” to the catalyst surface. Similar to Fig. 7, Fig. 9a shows that the increase in reaction rate is more profound at positive potentials. Fig. 9b shows that the variation of ρ with V_{WR} has the same shape as Δr versus V_{WR} . Either at positive or at negative values of V_{WR} , ρ initially increases with $|V_{WR}|$ until a plateau is reached, beyond which a minimal increase in ρ is observed. Fig. 9c shows that the effect of V_{WR} on $|A|$ is similar to that of $I/2F$ as shown in Fig. 8. Again, for the same $|V_{WR}|$, higher $|A|$ values are observed at positive currents.

Figs. 10a, b, and c show the same effects of V_{WR} on Δr , ρ , and $|A|$, respectively, using reactor R_3 instead of R_2 . It can be seen that the behavior is the same qualitatively, but not quantitatively. Much higher ρ and $|A|$ values are observed with R_3 . It should be pointed out that R_3 was the catalyst exposed to reaction conditions at 823 K for >72 h. Because of the long exposure to the reacting mixture at these temperatures, its catalytic activity was markedly reduced. This deactivation was attributed to carbon deposition on the Pt surface (Fig. 4). Hence catalyst R_3 exhibited poor open-circuit catalytic activity but a dramatic NEMCA effect.

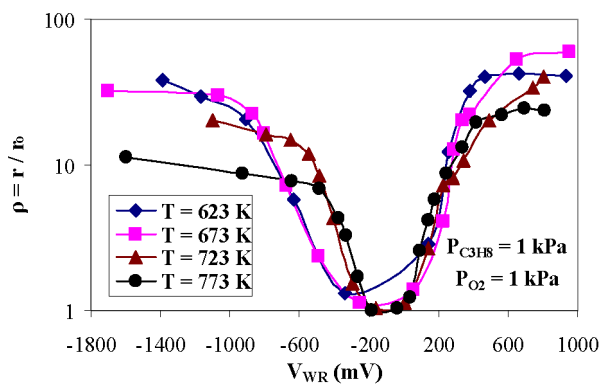
The effect of reactant composition on ρ and $|A|$ is shown in Figs. 11 and 12. Fig. 11 shows the effect of p_{O_2} on ρ and $|A|$ at positive overpotentials and for $p_{C_3H_8} = 1.0$ kPa. At $I = +20$ μ A, ρ and $|A|$ exhibit maxima at $p_{O_2} = 1.0$ kPa ($p_{O_2}/p_{C_3H_8} = 1$), whereas at $I = +400$ μ A, the maxima appears at $p_{O_2}/p_{C_3H_8} = 3$. The values of ρ are unusually high; ρ reaches 1400 at $I = +400$ μ A (Fig. 11a). Similarly, Fig. 12 shows the effect of p_{O_2} at negative overpotentials. Here the maxima on ρ and $|A|$ appear at $p_{O_2}/p_{C_3H_8} = 1$, for both $I = -20$ μ A and $I = -400$ μ A.

3.3. Oscillatory phenomena

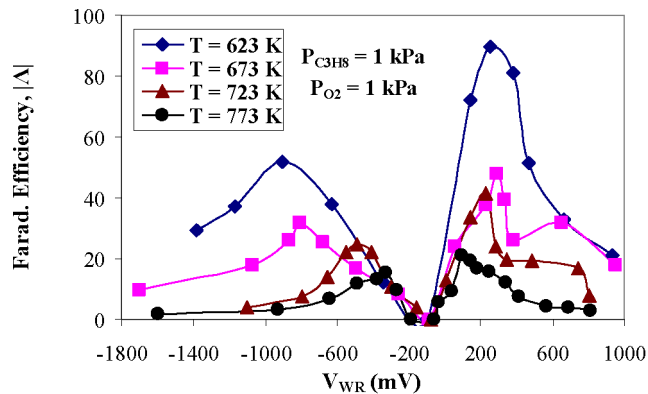
Fig. 13a shows reaction rate and SEP data obtained with reactor R_1 . The reactor operated under open circuit with the inlet composition kept at $p_{C_3H_8} = 1.4$ kPa and $p_{O_2} = 3.0$ kPa and temperature kept at 623 K. It can be seen that



(a)



(b)



(c)

Fig. 9. Effect of catalyst potential on (a) the induced increase in the rate of propane oxidation, (b) the rate enhancement ratio, ρ , and (c) the absolute Faradaic efficiency, $|A|$. $p_{C_3H_8} = 1$ kPa, $p_{O_2} = 1$ kPa, reactor R_2 .

both reaction rate ($r_{C_3H_8}$) and oxygen activity (α_o) exhibit multi-peaked oscillations. The period is about 17 min. Similarly, Fig. 13b shows the rate and surface oxygen activity behavior at 673 K and for the same inlet composition. Again, $r_{C_3H_8}$ and α_o oscillate with a period reduced to about 5 min.

Fig. 14 shows open- and closed-circuit results obtained with reactor R_2 . The inlet composition and the reactor temperature were kept constant ($p_{C_3H_8} = p_{O_2} = 1.0$ kPa, $T = 723$ K). Under open circuit, a steady-state rate of 5.2×10^{-10} mol/s is obtained (Fig. 14a). Under closed circuit and on imposing a current $I = 0.5$ mA, the rate increases to a new steady-state value of 5.6×10^{-9} mol/s (Fig. 14b). At

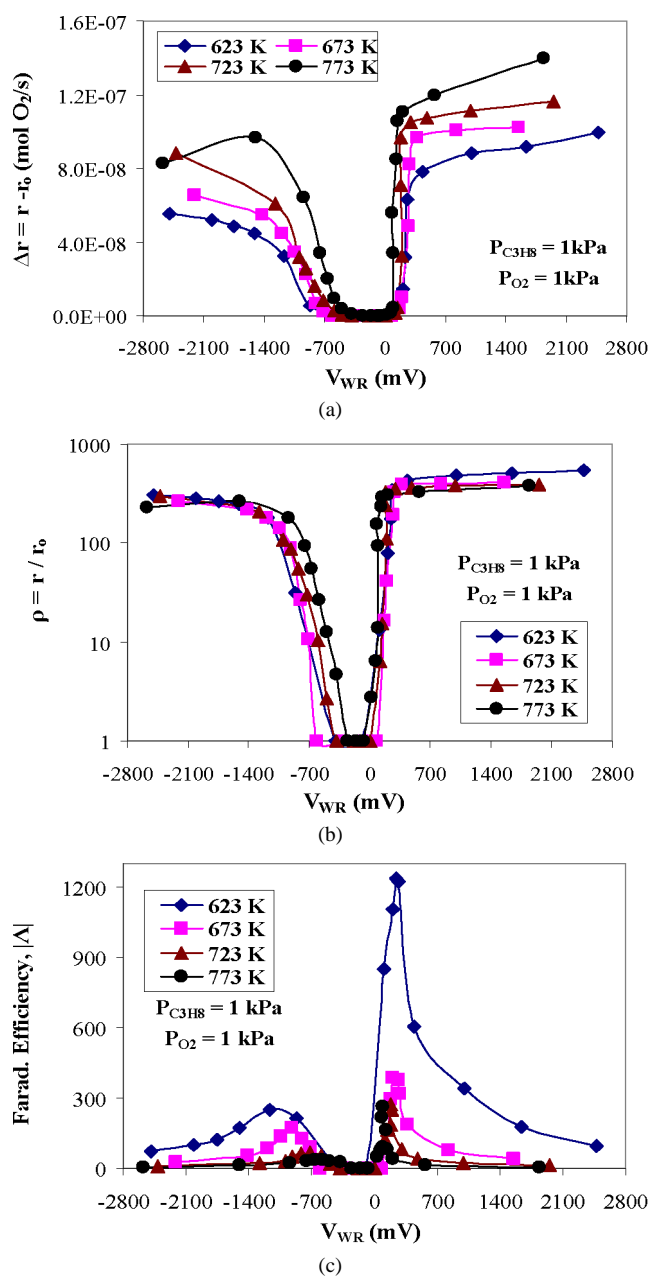


Fig. 10. Effect of catalyst potential on (a) the induced increase in the rate of propane oxidation, (b) the rate enhancement ratio, ρ , and (c) the absolute Faradaic efficiency, $|A|$. $p_{\text{C}_3\text{H}_8} = 1$ kPa, $p_{\text{O}_2} = 1$ kPa, reactor R₃.

higher currents, oscillatory behavior is observed, however. The period is about 9 min at $I = 1$ mA (Fig. 14c) and decreases to about 4.3 min at $I = 2$ mA (Fig. 14d) and 2.5 min at $I = 5$ mA (Fig. 14e).

4. Discussion

The kinetics of propane oxidation on Pt has been a stimulating problem for several decades [1–17,28,29]. Otto et al. [1] reported an apparent activation energy of 22 ± 3 kcal/mol, and apparent reaction orders of 0 for oxygen

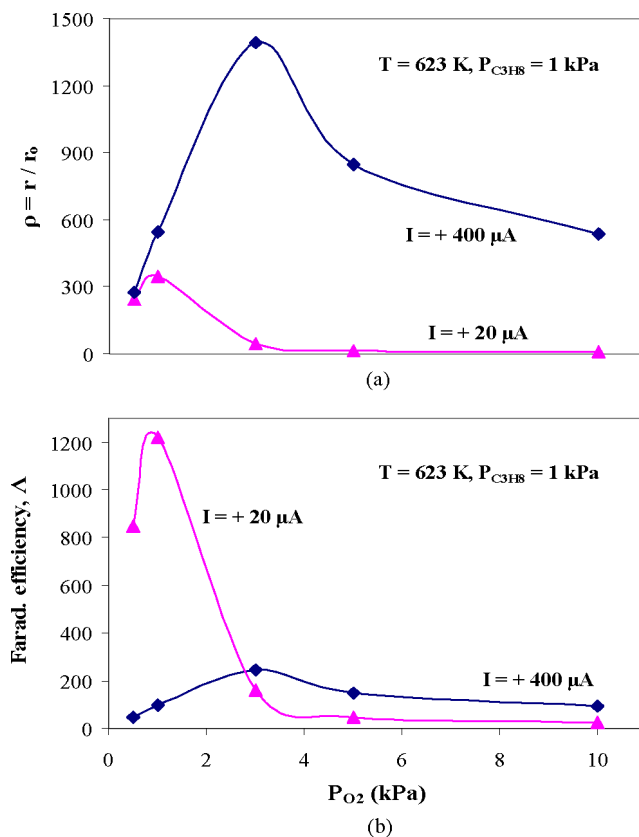


Fig. 11. Dependence of (a) ρ and (b) A , on the partial pressure of oxygen at positive currents. $T = 623$ K, $p_{\text{C}_3\text{H}_8} = 1$ kPa, reactor R₃.

and 1 for propane. Hubbard et al. [2] also found zero- and first-order dependence on oxygen and propane, respectively, and an apparent activation energy of 17.5 ± 3.5 kcal/mol. Garetto et al. [6] reported first-order dependence on propane with the reaction order for oxygen depending on the support used and varying from 0 to -1 . The apparent activation energy was also support-dependent and varied from 8.8 to 29 kcal/mol. Burch et al. [13] studied the effect of SO_2 on the catalytic activity of Pt/ Al_2O_3 and reported activation energies of 18.5 kcal/mol and 30 kcal/mol for untreated and sulfated catalysts, respectively. A first-order dependence on propane was found for both untreated and sulfated catalysts; for oxygen, the reaction order varied from -0.7 (untreated) to -1.5 (sulfated).

Vernoux et al. [20] used an experimental system very similar to the one used here to study and compare the NEMCA effects during propane and propylene oxidation. In addition to the closed-circuit results, they also examined the reaction under open circuit. Although they provided no details on the effect of $p_{\text{C}_3\text{H}_8}$, they reported on the role of p_{O_2} on the reaction rate. The oxygen content varied from 0.1 to 2.5% with temperature and propane content held constant at 673 K and 0.2%. The reaction rate was found to vary in a manner very similar to that shown in Fig. 6a; it went through a maximum at $p_{\text{O}_2}/p_{\text{C}_3\text{H}_8} = 1$, then decreased sharply to very low values exhibiting negative to zero-order kinetics. In the same work,

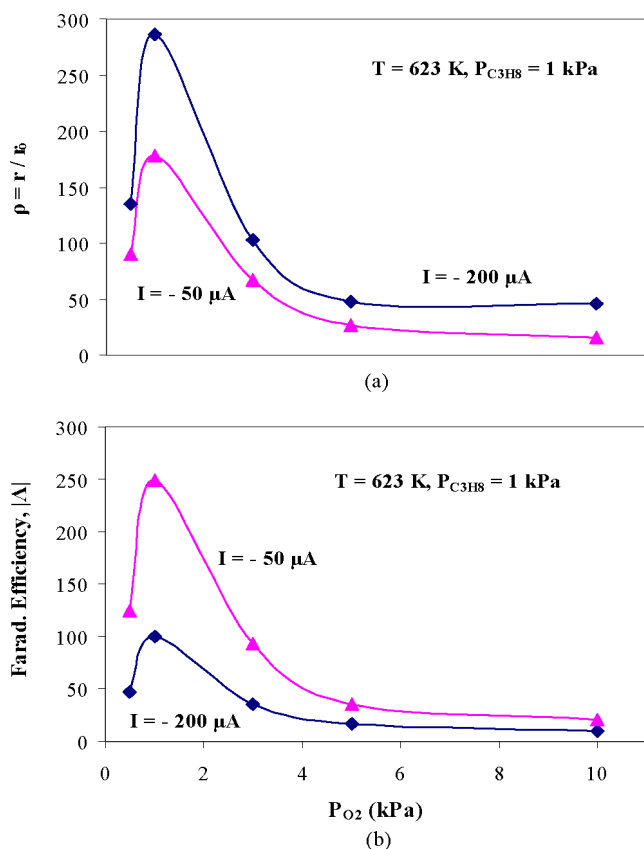


Fig. 12. Dependence of (a) ρ and (b) $|A|$, on the partial pressure of oxygen at negative currents. $T = 623$ K, $p_{\text{C}_3\text{H}_8} = 1$ kPa, reactor R₃.

the SEP technique was used to study the dependence of the open-circuit voltage of the cell on temperature. A smooth increase with increasing temperature was observed, with values varying from -170 mV at 545 K to about -65 mV at 680 K.

In the present study, the oxidation of propane was examined in view of the kinetic and potentiometric information obtained. Fig. 5a shows that, excluding the lowest temperature (623 K), the reaction order for propane is higher than 1. This seems to contradict findings of previous studies [1,2,6,13], which agree on linear dependence on propane. It should be pointed out, however, that in all of these studies, the reactant mixture was rich in oxygen. The oxygen:propane ratio varied from 5 to 50; that is, it was always above the stoichiometric. All of the data in Fig. 5 were obtained with $p_{\text{O}_2} = 3$ kPa; therefore, a comparison of the present results to those of earlier studies should be limited to values of $p_{\text{C}_3\text{H}_8} < 3$ kPa/5 = 0.6 kPa. Fig. 5a shows that the change in slope appears after $p_{\text{C}_3\text{H}_8}$ exceeds a temperature dependent value. These threshold $p_{\text{C}_3\text{H}_8}$ values are about 0.6 kPa ($p_{\text{O}_2}/p_{\text{C}_3\text{H}_8} = 5$) at 773 K, 0.85 kPa ($p_{\text{O}_2}/p_{\text{C}_3\text{H}_8} = 3.5$) at 723 K, and 1.4 kPa ($p_{\text{O}_2}/p_{\text{C}_3\text{H}_8} = 2.1$) at 673 K. Hence at all temperatures, the change in slope appears at propane-rich ratios, that is, $p_{\text{O}_2}/p_{\text{C}_3\text{H}_8} < 5$. Figs. 5a and b show that a change in the dependence of the reaction rate with $p_{\text{C}_3\text{H}_8}$ is accompanied by an analogous change in the

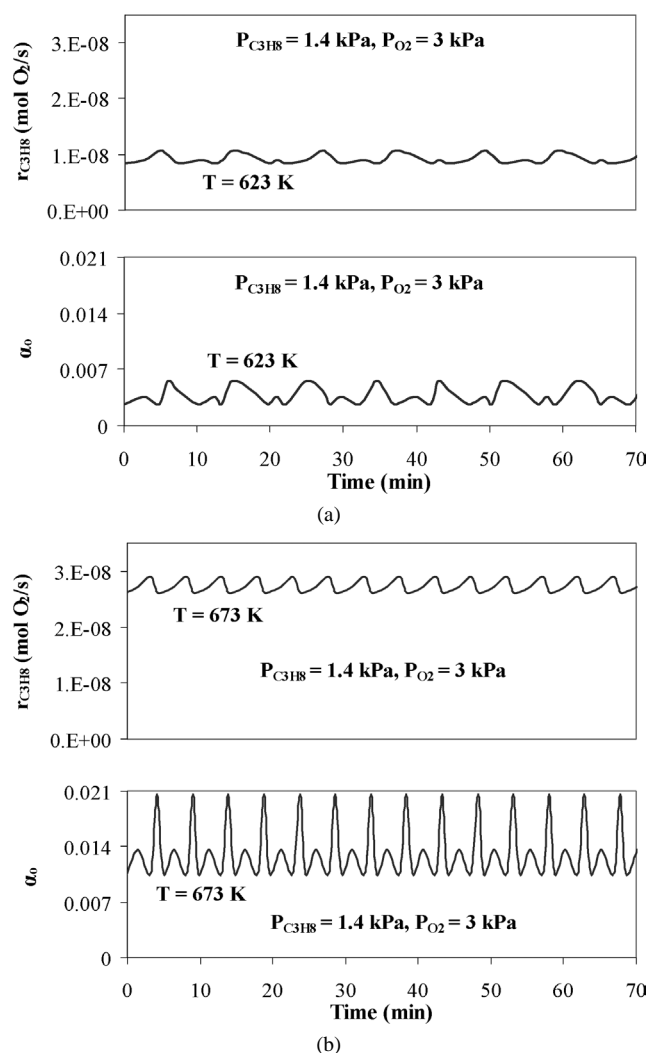


Fig. 13. Rate ($r_{\text{C}_3\text{H}_8}$) and oxygen activity (α_{O}) oscillations at (a) $T = 623$ K and (b) $T = 673$ K. $p_{\text{C}_3\text{H}_8} = 1.4$ kPa, $p_{\text{O}_2} = 3$ kPa, reactor R₁.

dependence of α_{O} . Within the low reaction rates region, the α_{O} values are up to one order of magnitude lower than their corresponding $p_{\text{O}_2}^{1/2}$ values, indicating a moderate deviation from thermodynamic equilibrium between adsorbed and gaseous oxygen. Within the high reaction rates regime, however, a strong deviation between α_{O} and $p_{\text{O}_2}^{1/2}$ is observed.

This type of behavior has been reported in two previous works in which kinetics were studied in conjunction with SEP measurements, namely the oxidation of hydrogen on Ni [26] and on Cu [27]. In those studies, the two regimes were associated with the oxidation of the catalyst and formation of surface oxide on which the reaction rate was significantly lower than on the reduced catalyst. This interpretation can apply to the present data as well. At high $p_{\text{O}_2}/p_{\text{C}_3\text{H}_8}$, the Pt surface is oxidized, and low reaction rates are attained. At low $p_{\text{O}_2}/p_{\text{C}_3\text{H}_8}$, the surface is reduced, making it much more active for propane oxidation. A high reaction rate means that the steady-state value of the thermodynamic activity of ad-

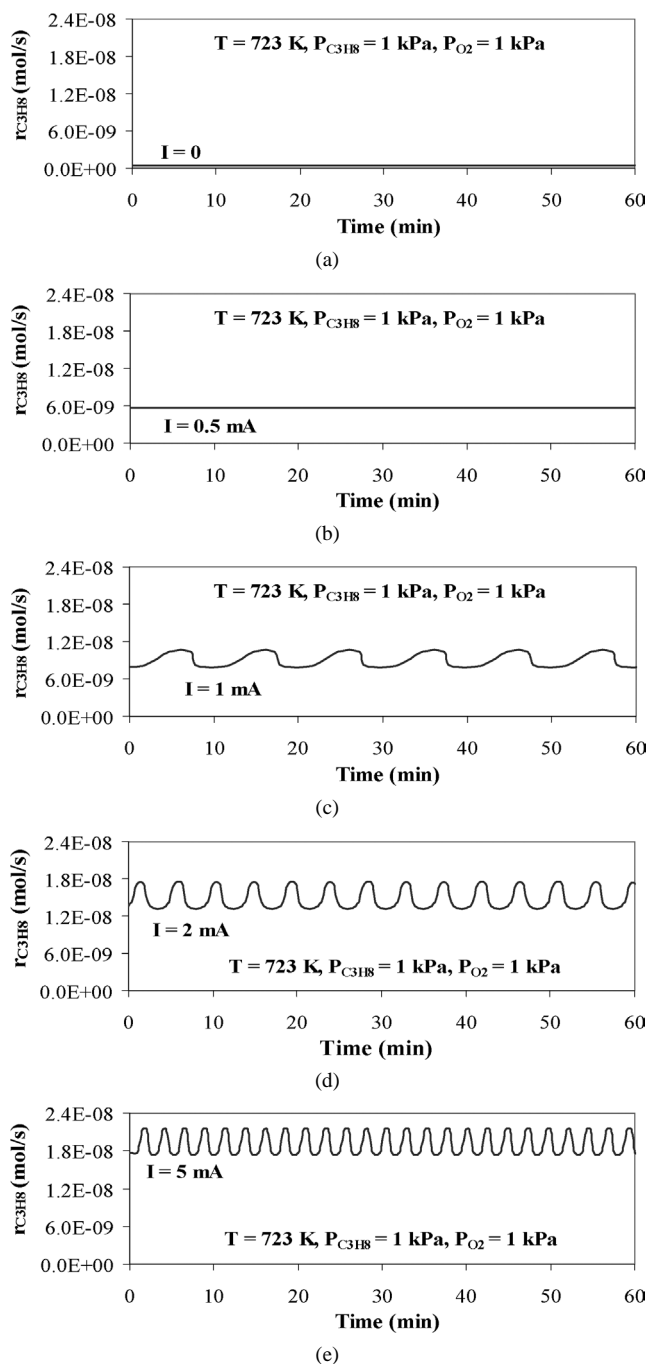


Fig. 14. Effect of applied current on the reaction rate: (a) $I = 0$, (b) $I = 0.5$ mA, (c) $I = 1$ mA, (d) $I = 2$ mA and (e) $I = 5$ mA. $T = 723$ K, $p_{\text{C}_3\text{H}_8} = 1$ kPa and $p_{\text{O}_2} = 1$ kPa, reactor R₂.

sorbed oxygen will be markedly reduced. This is shown on the right side of Fig. 5b, where, excluding the 623 K, α_o deviates from $p_{\text{O}_2}^{1/2}$ by two to five orders of magnitude. At the lowest temperature examined (623 K), the catalyst surface remains oxidized at all $p_{\text{C}_3\text{H}_8}$, and thus a linear reaction rate is observed.

The picture is quite similar in Fig. 6, which plots reaction rate and α_o versus p_{O_2} . At low p_{O_2} , the catalyst is reduced,

and high reaction rates are observed. As p_{O_2} increases, however, the Pt surface is gradually oxidized, and its catalytic activity drops. Hence, after going through a maximum, the rate decreases with p_{O_2} . At even higher p_{O_2} , the reaction rate tends to become independent of p_{O_2} . Again, Fig. 6b shows that α_o deviates significantly from its thermodynamic equilibrium value ($p_{\text{O}_2}^{1/2}$) in the reduced catalyst regime.

The experimental results presented in Figs. 5 and 6 indicate that, depending on the $p_{\text{O}_2}/p_{\text{C}_3\text{H}_8}$ ratio, each figure can be divided into two regions, one where the catalyst is reduced and very active and one in which the reaction rate is low and the catalyst is oxidized. If the data analysis is limited into the high $p_{\text{O}_2}/p_{\text{C}_3\text{H}_8}$ regime, then a linear dependence on $p_{\text{C}_3\text{H}_8}$ is observed (Fig. 5a). The apparent activation energy calculated from these data is 18.5 ± 2.5 kcal/mol. Similarly, the high $p_{\text{O}_2}/p_{\text{C}_3\text{H}_8}$ data of Fig. 6a show negative- to zero-order kinetics with respect to oxygen. The apparent activation energy extracted from these data should be the same as that calculated from Fig. 5a, and indeed, it was found to be 19.5 ± 2.5 kcal/mol. Thus the average value for the activation energy found herein is about 19 kcal/mol, which is in good agreement with those values reported in previous works [1,2,6,13].

Since 1981, when NEMCA was first observed during the oxidation of ethylene on Ag [30], this phenomenon has been studied in a very large number of heterogeneous catalytic systems [19]. The particular reaction of propane oxidation on Pt, has been studied by Vernoux et al. [20] and Kotsionopoulos and Bebelis [21]. Vernoux et al. compared the closed-circuit behavior of propane and propylene oxidation and found that propane exhibits electrophobic promotion; propylene, electrophilic promotion. The rate of propane oxidation was electrochemically enhanced on application of a positive voltage (O^{2-} pumped to the catalyst). Values as high as 2.3 for rate enhancement (ρ) and 1650 for Faradaic enhancement (Λ) were measured. On imposing negative voltages (O^{2-} pumped away from the catalyst), the catalytic rate was reduced by up to a factor of 3, with Λ attaining values as high as 14,250.

Kotsionopoulos and Bebelis studied the electrochemical promotion in the oxidation of propane on Pt and Rh at temperatures between 700 and 800 K [21]. On Pt, and at substoichiometric oxygen:propane ratios ($p_{\text{O}_2}/p_{\text{C}_3\text{H}_8} < 5$), the reaction rate was enhanced by either positive or negative overpotentials. The highest ρ measured were 1350 for positive overpotentials and 1130 for negative overpotentials.

The present NEMCA results are in qualitative agreement with those of Kotsionopoulos and Bebelis. Figs. 7–12 show that the reaction rate is enhanced electrochemically at both positive and negative overpotentials. This type of “inverted volcano” behavior has been observed in several NEMCA studies conducted on Ag, Au, Pd, Pt, and Rh catalysts [19]. On Pt, the inverted-volcano NEMCA has been observed in oxidation of methane [31], ethane [32], ethylene [33], propylene [34], and methanol [35]. The reaction exhibits elec-

trophobic behavior at positive potentials and electrophilic behavior at negative potentials.

The electrophobic behavior (i.e., the promoting effect at positive potentials) follows all of the NEMCA characteristics that were analyzed in detail by Vayenas et al. [18,19]. According to the classical interpretation, NEMCA is due to the electrochemically controlled backspillover of ionic species from the solid electrolyte to the catalyst electrode surface [19]. In the present study, on application of positive potentials, the back-spillover $O^{\delta-}$ species cause an increase in the catalyst work function, which in turn results in a weakening of the chemisorptive bond of oxygen. Noteworthy among the present results are the very high values of ρ , the reaction rate enhancement ratio, obtained especially with reactor R_3 . As mentioned earlier, R_3 is the catalyst that was gradually deactivated, resulting in a very low intrinsic catalytic activity (r_o). According to Eq. (3), ρ is inversely proportional to r_o . This can explain why the ρ values obtained with R_3 were much higher than those obtained with R_2 . In previous NEMCA studies, typical ρ values were between 5 and 50, and in only a few cases [19,36,37] have ρ values >100 been reported. In the recent work of Kotsionopoulos and Bebelis [21], the maximum ρ observed was 1350. Hence the value of 1400 observed in the present study (Fig. 11a) is the highest ever observed with any catalytic reaction system.

At negative potentials (i.e., on electrochemical removal of oxygen from the Pt surface), the reaction exhibits strong electrophilic behavior. Clearly, this type of electrochemical promotion cannot be attributed to ionic back-spillover. The interpretation of the observed rate increase can be similar to that reported by Kaloyiannis and Vayenas [18,32] for the oxidation of ethane on Pt. Thus at negative potentials, the promotion effect can be attributed to the electrochemically induced decrease in oxygen coverage and enhancement of propane chemisorption. In the present case, an additional factor may contribute to the rate enhancement: electrochemical “pumping” of oxygen away from the catalyst causes partial reduction of the surface and, consequently, an increase in reaction rate.

As mentioned earlier, the inverted-volcano type of NEMCA was also reported by Kotsionopoulos and Bebelis [21], but not by Vernoux et al. [20]. The latter focused primarily on the comparison between propane and propylene oxidation and found that the rate of propane oxidation increases at positive potentials but decreases at negative potentials. An explanation for this finding could be the different reaction conditions of the experiments. Vernoux et al.’s NEMCA experiments were done at 610–640 K, whereas ours done at 623–773 K. Also, Vernoux et al. worked at high oxygen: propane ratios ($5 < p_{O_2}/p_{C_3H_8} < 12$) whereas most of our NEMCA results, especially those with high ρ and Λ values, were obtained at $p_{O_2}/p_{C_3H_8} = 1$. It is possible that with reactor R_3 , the promotional effect on negative polarization is related to carbon deposition on the catalyst surface. Contributions from all of the aforementioned experimental details

may have been responsible for the differences between our results and results of Vernoux et al.

Figs. 13 and 14 show that under certain conditions, both reaction rate and surface oxygen activity exhibit oscillatory behavior. Since the discovery of oscillations in heterogeneous catalytic reactions in the late 1960s [38–40], numerous reaction systems have been reported to exhibit sustained oscillations. Several comprehensive reviews on this interesting subject have been published, and quite a few experimental and modelling details can be found therein [41–43]. The oxidation of propane is not listed as an oscillatory reaction in any of these reviews, however.

Recently, Gladky et al. reported oscillations during the catalytic oxidation of propane over a nickel wire [44]. The reaction was studied at 873–1123 K, and the reaction mixture was 95% propane and 5% oxygen. Oscillations were observed at 923–1023 K. The oscillation period was about 100 s, and the periodic changes in the reactant concentrations were accompanied by significant synchronous fluctuations in the catalyst temperature.

It is risky and inappropriate to consider that the oscillatory phenomena observed in the present work are necessarily of the same nature and origin as those reported by Gladky et al. Not only was the catalyst different in the two studies, but the experimental conditions were quite different as well. Gladky et al. used a high excess of propane (inlet $p_{O_2}/p_{C_3H_8} = 0.053$) and as a result detected products of partial oxidation, such as H_2 , in the effluent stream. The concentration of H_2 was found to oscillate together with the concentrations of O_2 and H_2O [44].

For the data exhibiting oscillations (Fig. 13), the conversion of propane and oxygen was low (<8%). The catalyst temperature remained constant during the oscillations. Given the accuracy of the measurement, it is certain that the temperature could not fluctuate by more than 2–3 K. If the observed changes in the reaction rate were due to changes of the catalyst temperature only, then the latter should be about 15–20 K; therefore, the present oscillations are not of thermal origin.

Oscillations have been observed in the catalytic oxidation of C_3H_6 , CO, and H_2 on Pt [41–43]. If any of these compounds were among the products, then one could assume that the observed oscillatory phenomena are related to the oxidation of that compound rather than to the oxidation of propane. But none of these products was detected here. In particular, the absence of CO, reported to be an intermediate of either the partial or the deep oxidation of propane [17], was verified by both the gas chromatography measurements and the infrared CO analysis. It is possible that the observed oscillations are related to periodic oxidation and reduction of the catalyst surface. This assumption is partially supported by the closed-circuit results of Fig. 14. The open-circuit catalytic reaction rate exhibits a stable steady state, but with increasing catalyst potential, the rate eventually becomes oscillatory.

A conclusive interpretation of the phenomena observed in the present study requires further experimental work. Specifically, the limits of gas phase composition and temperature, within which sustained oscillations appear, need to be investigated. Experimental work in this direction is currently in progress.

5. Conclusions

The catalytic oxidation of propane on Pt was studied under both open-circuit and closed-circuit conditions. With the cell operating at open circuit, the reaction was positive order in propane and, depending on the $p_{O_2}/p_{C_3H_8}$ ratio, either first, zero, or negative order in oxygen. The apparent activation energy was about 19 kcal/mol. Under certain conditions, reaction rate and surface oxygen activity exhibited sustained oscillations.

With the cell operating at closed circuit, the reaction exhibited a strong NEMCA effect of the “inverted volcano” type; that is, the rate is electrochemically promoted at either positive or negative potentials. At positive potentials, the effect is more pronounced, and the intrinsic reaction rate can be enhanced by up to a factor of 1400. On imposing a constant potential, it is possible to electrochemically induce oscillations in the reaction rate.

Acknowledgment

The authors acknowledge financial support for this research from the Chemical Process Engineering Research Institute (CPERI) of Thessaloniki.

References

- [1] K. Otto, J.M. Andino, C.L. Parks, *J. Catal.* 131 (1991) 243.
- [2] C.P. Hubbard, K. Otto, H.S. Gandhi, K.Y.S. Ng, *J. Catal.* 139 (1993) 268.
- [3] A.F. Lee, K. Wilson, R.M. Lambert, C.P. Hubbard, R.G. Hurley, R.W. McCabe, H.S. Gandhi, *J. Catal.* 184 (1999) 491.
- [4] L. Kiwi-Minsker, I. Yuranov, E. Slavinskaja, V. Zaikovskii, A. Renken, *Catal. Today* 59 (2000) 61.
- [5] Y. Yazawa, N. Takagi, H. Yoshida, S. Komai, A. Satsuma, T. Tanaka, S. Yoshida, T. Hattori, *Appl. Catal. A* 233 (2002) 103.
- [6] T.F. Garetto, E. Rincón, C.R. Apestegua, *Appl. Catal. B* 48 (2004) 167.
- [7] M. Huff, L.D. Schmidt, *J. Catal.* 149 (1994) 127.
- [8] A. Beretta, L. Piovesan, P. Forzatti, *J. Catal.* 184 (1999) 455.
- [9] A. Beretta, P. Forzatti, E. Ranzi, *J. Catal.* 184 (1999) 469.
- [10] H. Yoshida, Y. Yazawa, T. Hattori, *Catal. Today* 87 (2003) 19.
- [11] Y. Yazawa, H. Yoshida, T. Hattori, *Appl. Catal. A* 237 (2002) 139.
- [12] A. Ishikawa, S. Komai, A. Satsuma, T. Hattori, Y. Murakami, *Appl. Catal. A* 110 (1994) 61.
- [13] R. Burch, E. Halpin, M. Hayes, K. Ruth, J.A. Sullivan, *Appl. Catal. B* 19 (1998) 199.
- [14] C.P. Hubbard, K. Otto, H.S. Gandhi, K.Y.S. Ng, *J. Catal.* 144 (1993) 484.
- [15] H. Wu, L. Liu, S. Yang, *Appl. Catal. A* 211 (2001) 159.
- [16] Y. Yazawa, H. Yoshida, S. Komai, T. Hattori, *Appl. Catal. A* 233 (2002) 113.
- [17] A. Hinz, M. Skoglundh, E. Fridell, A. Anderson, *J. Catal.* 201 (2001) 247.
- [18] C.G. Vayenas, M.M. Jaksic, S. Bebelis, S.G. Neophytides, in: J.O'.M. Bockris, B.E. Conway, W.R.E. White (Eds.), *The Electrochemical Activation of Catalytic Reactions*, in: *Modern Aspects in Electrochemistry*, vol. 29, Plenum, 1996, p. 57.
- [19] C.G. Vayenas, S. Bebelis, C. Pliangos, S. Brosda, D. Tsiplakides, *Electrochemical Activation of Catalysis*, Kluwer Academic/Plenum, New York, 2001.
- [20] P. Vernoux, F. Gaillard, L. Bultel, E. Siebert, M. Primet, *J. Catal.* 208 (2002) 412.
- [21] N. Kotsionopoulos, S. Bebelis, Presented at the 55th Annual Meeting of the International Society of Electrochemistry, Thessaloniki, Greece (Sept. 19–24, 2004), paper No. S11FP48.
- [22] M. Estenfelder, T. Hahn, H.-G. Lintz, *Catal. Rev.-Sci. Eng.* 46 (2004) 1.
- [23] M. Stoukides, *Catal. Rev.-Sci. Eng.* 42 (2000) 1.
- [24] C. Wagner, *Adv. Catal.* 21 (1970) 323.
- [25] C.G. Vayenas, H. Saltsburg, *J. Catal.* 57 (1979) 296.
- [26] C. Saranteas, M. Stoukides, *J. Catal.* 93 (1985) 417.
- [27] A. Balian, G. Hatzigiannis, D. Eng, M. Stoukides, *J. Catal.* 145 (1994) 526.
- [28] A. Schwartz, L.L. Holbrook, H. Wise, *J. Catal.* 21 (1971) 199.
- [29] H.C. Yao, H.K. Stepien, H.S. Gandhi, *J. Catal.* 67 (1981) 231.
- [30] M. Stoukides, C.G. Vayenas, *J. Catal.* 70 (1981) 130.
- [31] P. Tsiakaras, C.G. Vayenas, *J. Catal.* 140 (1993) 53.
- [32] A. Kaloyiannis, C.G. Vayenas, *J. Catal.* 171 (1997) 148.
- [33] C. Pliangos, I.V. Yentekakis, S. Ladas, C.G. Vayenas, *J. Catal.* 159 (1996) 189.
- [34] P. Beatrice, C. Pliangos, W.L. Worrell, C.G. Vayenas, *Solid State Ionics* 136–137 (2000) 833.
- [35] C.G. Vayenas, S. Neophytides, *J. Catal.* 127 (1991) 645.
- [36] S. Wodiunig, C. Comminellis, *J. Eur. Ceram. Soc.* 19 (1999) 931.
- [37] C. Pliangos, C. Raptis, T. Badas, C.G. Vayenas, *Solid State Ionics* 136–137 (2000) 767.
- [38] P. Hugo, in: *Fourth European Symposium on Chemical Reaction Engineering*, Brussels, 1968, Pergamon, Oxford, 1971, p. 459.
- [39] P. Hugo, *Ber. Bunsen-Ges. Phys. Chem.* 74 (1970) 121.
- [40] E. Wicke, H. Beusch, P. Fieguth, *ACS Symp. Ser.* 109 (1972) 615.
- [41] M.M. Slin'ko, N.I. Jaeger, in: B. Delmon, J.T. Yates (Eds.), *Studies in Surface Science and Catalysis*, vol. 86, Elsevier, Amsterdam, 1994.
- [42] F. Shuth, B.E. Henry, L.D. Schmidt, *Adv. Catal.* 39 (1993) 51.
- [43] R. Imbihl, G. Ertl, *Chem. Rev.* 95 (1995) 697.
- [44] A.Yu. Gladky, V.K. Ermolaev, V.N. Parmon, *Catal. Lett.* 77 (2001) 103.